Temperature-responsive biometamaterials for gastrointestinal applications

DRUG DELIVERY

Temperature-responsive biometamaterials for gastrointestinal applications

Sahab Babaee[1], Simo Pajovic[1], Ameya R. Kirtane[1], Jiuyun Shi[1], Ester Caffarel-Salvador[1,2], Kaitlyn Hess[1], Joy E. Collins[1], Siddartha Tamang[1], Aniket V. Wahane[1], Alison M. Hayward[1,3], Hormoz Mazdiyasni[1,4], Robert Langer[1,2]*, Giovanni Traverso[1,4,5]*

We hypothesized that ingested warm fluids could act as triggers for biomedical devices. We investigated heat dissipation throughout the upper gastrointestinal (GI) tract by administering warm (55°C) water to pigs and identified two zones in which thermal actuation could be applied: esophageal (actuation through warm water ingestion) and extra-esophageal (protected from ingestion of warm liquids and actuatable by endoscopically administered warm fluids). Inspired by a blooming flower, we developed a capsule-sized esophageal system that deploys using elastomeric elements and then recovers its original shape in response to thermal triggering of shape-memory nitinol springs by ingestion of warm water. Degradable millineedles incorporated into the system could deliver model molecules to the esophagus. For the extra-esophageal compartment, we developed a highly flexible macrostructure (mechanical metamaterial) that deforms into a cylindrical shape to safely pass through the esophagus and deploys into a fenestrated spherical shape in the stomach, capable of residing safely in the gastric cavity for weeks. The macrostructure uses thermoresponsive elements that dissociate when triggered with the endoscopic application of warm (55°C) water, allowing safe passage of the components through the GI tract. Our gastric-resident platform acts as a gram-level long-lasting drug delivery dosage form, releasing small-molecule drugs for 2 weeks. We anticipate that temperature-triggered systems could usher the development of the next generation of stents, drug delivery, and sensing systems housed in the GI tract.

INTRODUCTION

Warm fluids have been consumed since antiquity (*1*). Their ingestion and preferences with respect to temperature have established a predilection for warm beverages between 55° and 70°C and even up to 78.5°C (*2*). Hot fluid ingestion has been associated with a potential increase in cancer, leading the International Agency for Research on Cancer to classify hot fluids (>65°C) as probably carcinogenic to humans (*3*); however, temperatures between 55° and 65°C have been identified as an ideal temperature range associated with a satisfactory sensation to the consumer without burning and harmful effects (*4*, *5*). Although considerable work has been undertaken to understand the potential carcinogenic effects of the ingestion of hot fluids, less is understood about the dynamics of heat dissipation of warm fluids (≤55°C) throughout the esophagus and stomach. Here, we describe experiments in a large animal model that define anatomical, temporal, and thermal boundary conditions in the upper gastrointestinal (GI) tract obtained upon ingestion of warm fluids outside the carcinogenic temperature range.

GI devices are being applied broadly across clinical indications ranging from cancer (stents and percutaneous gastrostomy tubes) and bariatrics (balloons) to systems for drug delivery and long-term energy harvesting (*6*–*9*). Having triggerable control over such systems—exploiting light-, pH-, magnetic-, and solvent-responsive materials (*10*–*13*)—can impart greater functionality over the system's residency, drug release, and other behaviors. However, all of these approaches are restricted to slow response, which is a major drawback for many potential applications. Using temperature-responsive components with an ultrafast and robust response enables development of a new generation of ultra-responsive GI devices. Here, we report the characterization of warm fluid heat dissipation in a large animal model. We further report the development of an esophageal system that can be applied to drug delivery, supported by ex vivo data, and detail multiweek drug delivery in vivo using a macro-gastric resident system in a large animal model. These two systems exemplify the application of the differential temperature dissipation observed in the esophageal and extra-esophageal compartments.

The capacity of macrosystems to reside safely in the GI tract offers a broad set of opportunities including ones for sensing (*14*) and therapy (*7*, *8*). For example, macrodevices have the potential to house large drug depots (in the multigram range) for the treatment of infections and other conditions requiring prolonged therapy. Moreover, macrosystems can be imparted with electrical capabilities to sense a range of signals to facilitate mobile health and the monitoring of patients suffering from chronic conditions where early detection of a signal such as bleeding or a fever could considerably enhance our capacity to intervene (*15*). The removal of such devices requires interventions and extraction from the gastric cavity, which have been associated with significant morbidity including GI perforation (*16*). The incorporation of temperature-triggered systems stands to enhance the potential safety by facilitating the breakdown of a macrodevice into smaller segments that can be excreted.

RESULTS

In vivo evaluation of heat dissipation in upper GI tract

We characterized temperature changes across the upper GI tract using a fabricated temperature testing setup made of thermocouple probes

[1]Department of Chemical Engineering and Koch Institute for Integrative Cancer Research, Massachusetts Institute of Technology, Cambridge, MA 02139, USA. [2]Institute for Medical Engineering and Science, Massachusetts Institute of Technology, Cambridge, MA 02139, USA. [3]Division of Comparative Medicine, Massachusetts Institute of Technology, Cambridge, MA 02139, USA. [4]Department of Mechanical Engineering, Massachusetts Institute of Technology, Cambridge, MA 02139, USA. [5]Division of Gastroenterology, Brigham and Women's Hospital, Harvard Medical School, Boston, MA 02115, USA.
*Corresponding author. Email: rlanger@mit.edu (R.L.); ctraverso@bwh.harvard.edu, cgt20@mit.edu (G.T.)

upon administration of warm water (55°C) at different volumes and rates to pigs in the seated position, mimicking the orientation of the human GI tract while drinking (Fig. 1A, fig. S1, and the "In vivo temperature testing" section). The accuracy and repeatability of the probes were confirmed in vitro (fig. S2). Figure 1B shows an example of temperature decay in the upper GI tract upon ingestion of 100 ml of 55°C water during a 10-s administration period (steady-state flow rate). The temperature rose to about 50°C in the upper esophagus, 48°C in the middle esophagus, and 45°C in the lower esophagus. However, no temperature change was detected in the stomach, indicating complete dissipation of heat over the length of the esophagus. The change in upper GI tract temperature (ΔT) was recorded for increasing volumes of water at 55°C (Fig. 1C). Data in Fig. 1 (B and C) confirmed that temperature could be controlled in the esophagus (probes 1 to 6) and in the proximal stomach (probes 7 and 8) using high volumes of 55°C warm water (100, 200, and 250 ml). Low volumes of the warm water (10 and 20 ml) in the range of a single gulp (*17*) manifested in minimal temperature changes, supporting the idea that accidental actuation of thermoresponsive elements through daily consumption of hot beverages is unlikely. The temperature change was negligible in the bulk of the stomach (probes 9 to 16) regardless of the volume ingested, establishing two zones with differential responses to the warm fluids: the esophageal zone (responsive to the ingestible warm fluids) and the extra-esophageal zone (nonresponsive to ingestion of warm fluids).

For the two zones identified, we developed and evaluated two temperature-triggerable technologies: (i) a flower-like system, inspired by the construction and motion of a blooming flower, that can be thermally actuated via oral administration of a warm liquid for delivery of therapeutics through millineedles to the esophageal mucosa and (ii) a highly reconfigurable mechanical metamaterial (macrostructure dosage form) for prolonged large-dose gastric drug delivery that can be triggered via spraying warm fluids endoscopically. Each prototype used different thermoresponsive elements in its construction. The flower-like system uses a shape-memory alloy that enables shape change upon temperature-based triggering, whereas the macrostructure uses a thermosensitive polymer weakened by change in temperature over its glass transition temperature.

Design and evaluation of an esophageal flower-like system

The schematic and prototype images of a flower-like system showing the sequence of deployment and thermally triggered configurations are illustrated in Fig. 2. It consists of a temperature-triggerable multimaterial prototype made of four polymeric arms [made from poly(ε-caprolactone) or PCL] connected to a central PCL core through four elastic L-beam–shaped recoil elements (Elastollan 1185A; fig. S3). These elastic elements provided the required force for deployment through trapped elastic energy in the elastic L-beams during folding. Four nickel-titanium (nitinol) wires set to torsion springs were incorporated into the design to enable the temperature triggering and closure of the prototype (Fig. 3A and fig. S4).

Nitinol is a well-recognized, biocompatible alloy suitable for biomedical applications (*18*) that has a unique property: It can undergo a phase transformation in its crystal structure accompanied by an increase in elastic modulus at the transition temperature (T_c). Thus, torsion springs (created by heat treatment of the nitinol wires; fig. S5)

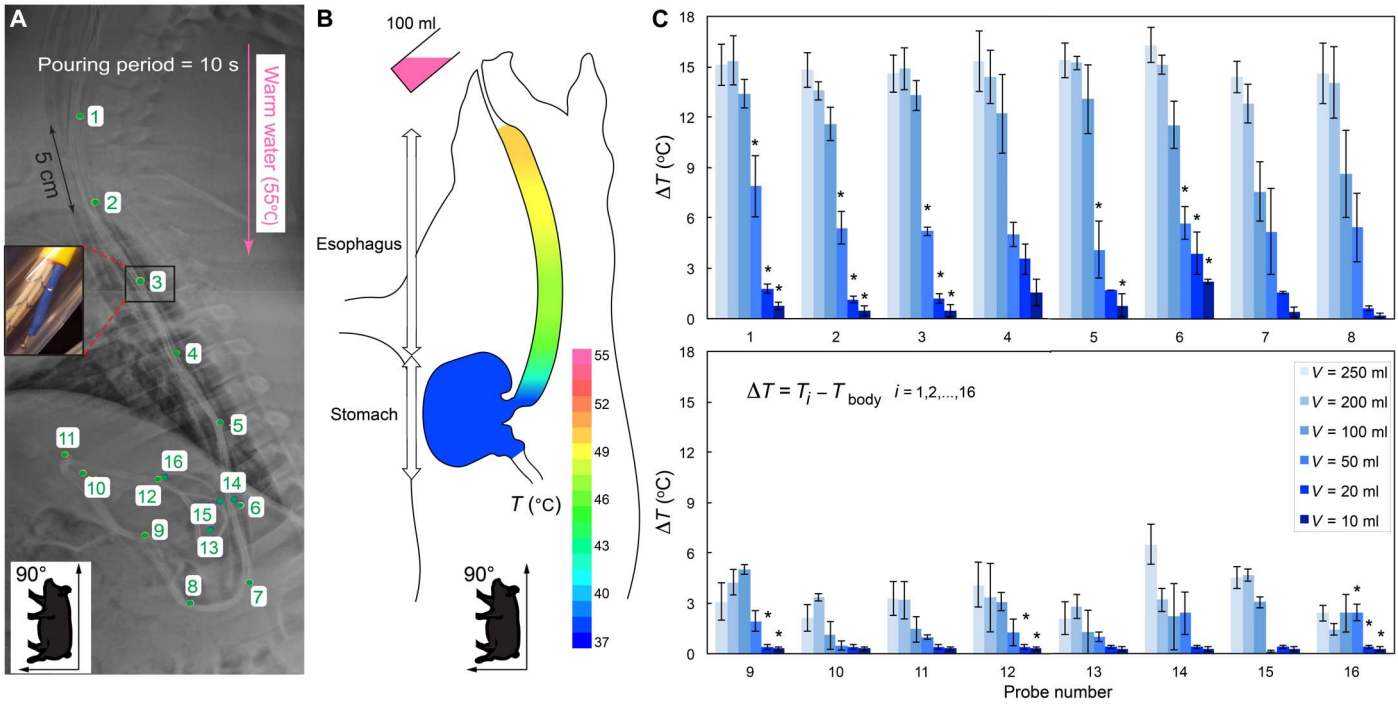

Fig. 1. In vivo evaluation of heat dissipation in the upper GI tract. (**A**) A radiograph showing the position of the 16 temperature probes (green numbers indicate K-type thermocouples, shown magnified in the inset) arranged in the esophagus and stomach of a Yorkshire pig secured in seated position. The pink arrow indicates direction of water delivery. (**B**) Schematic depicting temperature decay in the upper GI tract when 100 ml of 55°C water (pseudocolored pink) was orally administered. (**C**) Temperature changes (ΔT) in the upper GI tract during administration of 55°C volumes of water [V = 10, 20, 50, 100, 200, and 250 ml] in 10 s as a function of probe number i, i = 1, 2, …, 16, as shown in (A). Data are reported as means ± SD for n = 3 measurements for each group. *P < 0.05 (versus V = 100 ml at corresponding probe by one-way analysis of variance (ANOVA)].

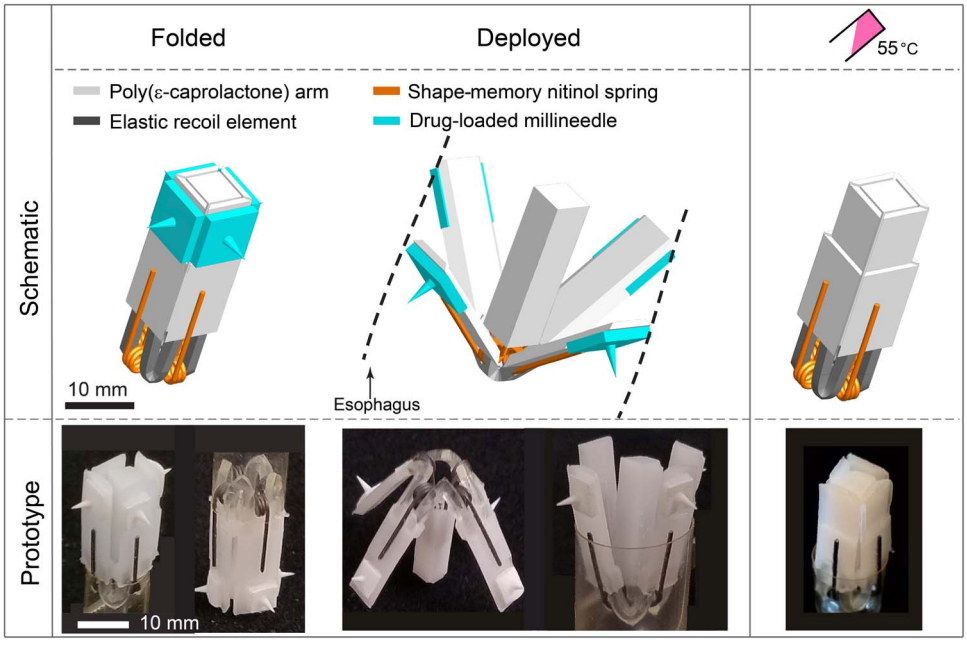

Fig. 2. Esophageal flower-like system. Schematic and prototype images of the flower-like system, illustrating the configurations when folded (before administration), deployed in the esophagus, and folded again following temperature triggering. The components of the design including polymeric arms (light gray), elastic recoil elements (dark gray), nitinol springs (orange), and dissoluble millineedles (green) are shown.

have greater recoiling forces upon triggering at T_c = 50°C. The key design challenge is to satisfy the following inequality

$$F_{cr}^{nitinol}(\text{at } T < T_c) < F_{cr}^{Elastollan} < F_{cr}^{nitinol}(\text{at } T \geq T_c)$$

where $F_{cr}^{nitinol}$ and $F_{cr}^{Elastollan}$ are the nitinol spring and elastic element (Elastollan 1185A) recoiling forces as a function of the temperature T, respectively, and T_c = 50°C is the nominal transition temperature of the nitinol. This guarantees robust deployment (opening) due to elasticity of the elastic elements at body temperature ($T < T_c$) and closure (folding) in response to thermal triggering of the nitinol springs ($T \geq T_c$), which can be achieved by controlling spring design parameters. Considering a constant spring wire diameter (ϕ = 0.5 mm due to manufacturing limitations) and arm length (10 mm), coil diameter (d) and number of coils (n) represent a two-dimensional (2D) design space, which allowed us to carry out a systematic experimental study on the effect of d and n on $F_{cr}^{nitinol}$ (Fig. 3B, fig. S6, and the "Mechanical characterization of the flower-like prototype" section). The blue area represents the experimentally observed valid design space. The torsion springs of d = 2 mm and n = 2.5 mm were selected as optimal design to assemble the final prototype.

To confirm the chosen design parameters, we tested the flower-like prototype in vivo in pigs. Upon releasing in the upper esophagus, the prototype rapidly deployed because of elastic energy trapped in the elastic elements during folding, enabling contact of the four arms with the esophageal wall (Fig. 3C). To thermally trigger the exit of the prototype from the esophagus, we administered 100 ml of 55°C water, which increased the temperature in the esophagus by $\Delta T \sim 13$°C to reach the approximate transition temperature of the springs (T_c = 50°C). This led to full closure of the prototype (movies S1 and S2) and its subsequent passage from the esophagus into the stomach.

To enable drug loading and delivery with the flower-like system, we mounted polymeric millineedles capable of penetrating the esophageal mucosa without perforation (Fig. 3, D and E) on the outer side of the device arms (fig. S7). A macromolecule (fluorescently labeled dextran) or a small molecule (budesonide) loaded into the tips of the millineedles was delivered ex vivo in three porcine esophagi using the prototypes (Fig. 3, F and G), further supporting the potential for this drug delivery system to administer agents to the GI tract (the "Ex vivo testing of the flower-like prototype" section).

Flexible mechanical metamaterial as a macrostructure dosage form

Inspired by the need for reconfigurable and adaptive materials capable of targeted and extreme volume changes (*19*–*22*), we designed a mechanical metamaterial (architected material) with highly tunable shape and volume that could be deployed endoscopically in the extra-esophageal zone (Fig. 4). This highly foldable metamaterial, so-called macrostructure dosage form, is a multimaterial design composed of three components: (i) semirigid arms to carry therapeutic agents, (ii) elastic hinges to provide flexibility of the dosage form, and (iii) thermoresponsive linkers (TRLs) for disassembly and safe passage. This can be used as a platform for housing large depots of therapeutic payload for extended release over the course of several weeks. Because of the lack of responsiveness of the stomach to ingested warm fluids, the structure can be triggered by local administration of warm fluids. The reconfigurable behavior and foldability of the metamaterials offer two advantages: (i) considerable compaction under compression that ensures the safe delivery of metamaterials and large loaded drug depots through narrow orifices in the digestive system, such as the esophagus, and (ii) expansion inside the stomach to achieve prolonged retention and prevent exiting through the pylorus while allowing the passage of food.

The macrostructure consists of 24 arms (length, 50 mm) with square cross sections (2.6 mm × 2.6 mm), which are joined through elastic hinges (fig. S8). The semirigid polymeric arms serve as a drug delivery matrix to carry large loads of drugs, providing controlled release for long periods (weeks) and structural integrity to the dosage form. The arms are joined through elastic hinges at the corners and mid-edges of the macrostructure. Arms are made of two segments, each 25 mm long, connected through TRLs and mechanically mated (fig. S8). The elastic hinges enable the macrostructure dosage form to be deformed to a shape and size that can be safely passed through the esophagus and expanded in the stomach, where the device adopts a fenestrated spherical shape (Fig. 4). The TRLs can be weakened by endoscopically spraying with warm water (T = 55°C) but remain stable in the acidic gastric environment. The 24 thermal linkers (Fig. 4) are wrapped around the arm segments to provide stability and integrity of the macrostructure. Thermal linkers are weakened upon spraying with 55°C water, causing the macrostructure to be disintegrated into small fragments in a predictable manner that can exit the

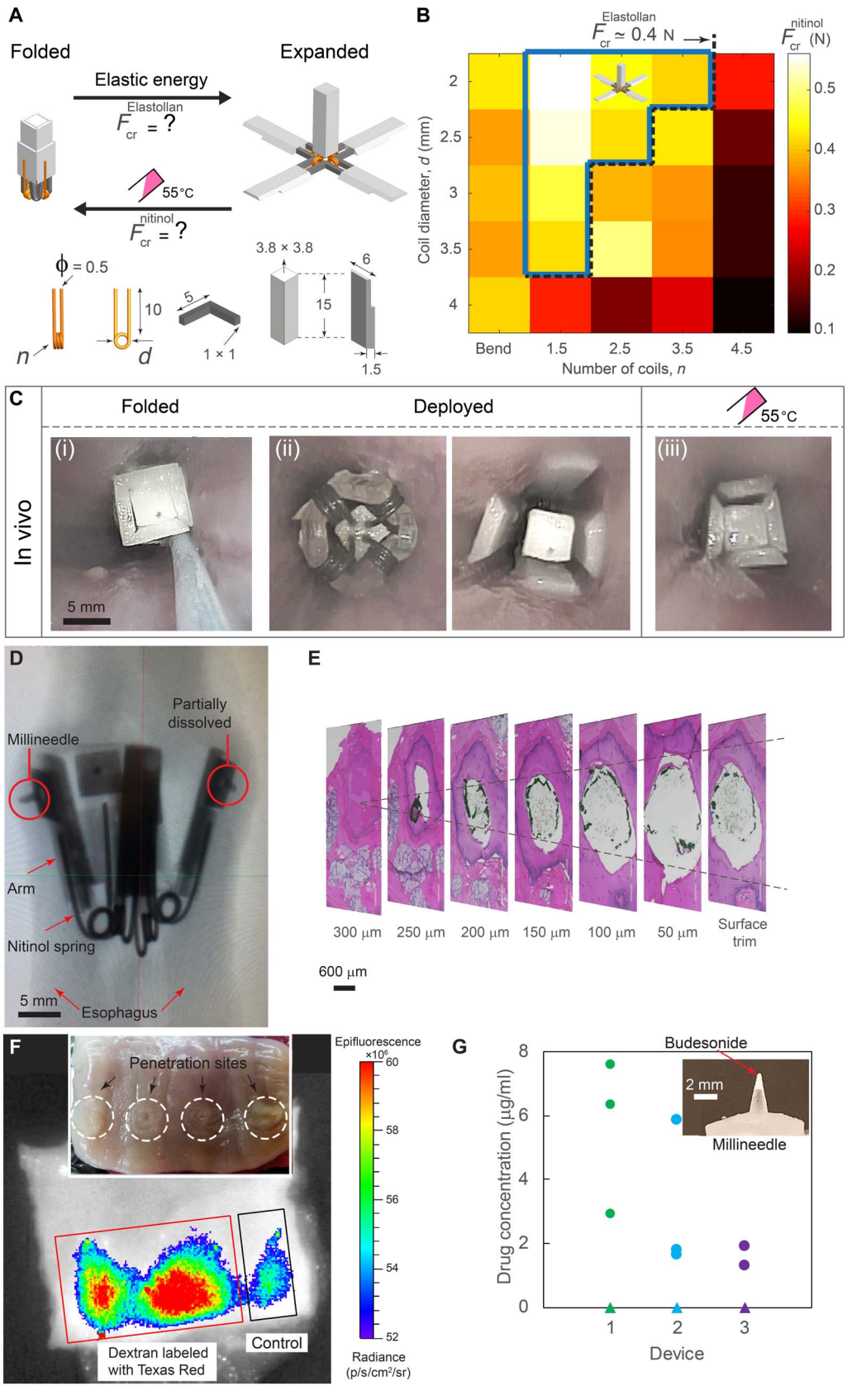

Fig. 3. Mechanical characterization, in vivo deployment, and ex vivo evaluation of the flower-like prototype. (**A**) Schematic depicting transformable folded and expanded configurations and corresponding recoiling forces of the elastic elements ($F_{cr}^{Elastollan}$) and the nitinol springs ($F_{cr}^{nitinol}$). The dimensions of the prototype are shown in millimeters. $F_{cr}^{nitinol}$ for nitinol springs with a wire diameter ϕ = 0.5 mm reported for differing number of coils (n) and coil diameters (d) in (**B**). The dashed black line represents $F_{cr}^{Elastollan} = 0.4$ N for a given dimension of the prototype. The blue area represents the experimentally observed valid design space. (**C**) In vivo endoscopic images of the prototype in pig's esophagus in different configurations: (i) folded, (ii) deployed in direct and reverse directions, and (iii) folded after administration of 100 ml of 55°C water. (**D**) Radiograph and (**E**) histology results indicating penetration and dissolution of millineedles. (**F**) IVIS (in vivo imaging system) visualization of millineedle-administered dextran fluorescence in esophageal tissue. The control needle was devoid of dextran. The inset shows the optical image of the penetration sites highlighted with white circles. (**G**) Concentration of budesonide delivered to the esophageal tissue for n = 3 prototypes [each prototype is shown by a different color and consisted of one control needle (triangle) and three drug-loaded needles (circles)]. The inset shows a millineedle loaded with 0.1 mg of budesonide at the tip.

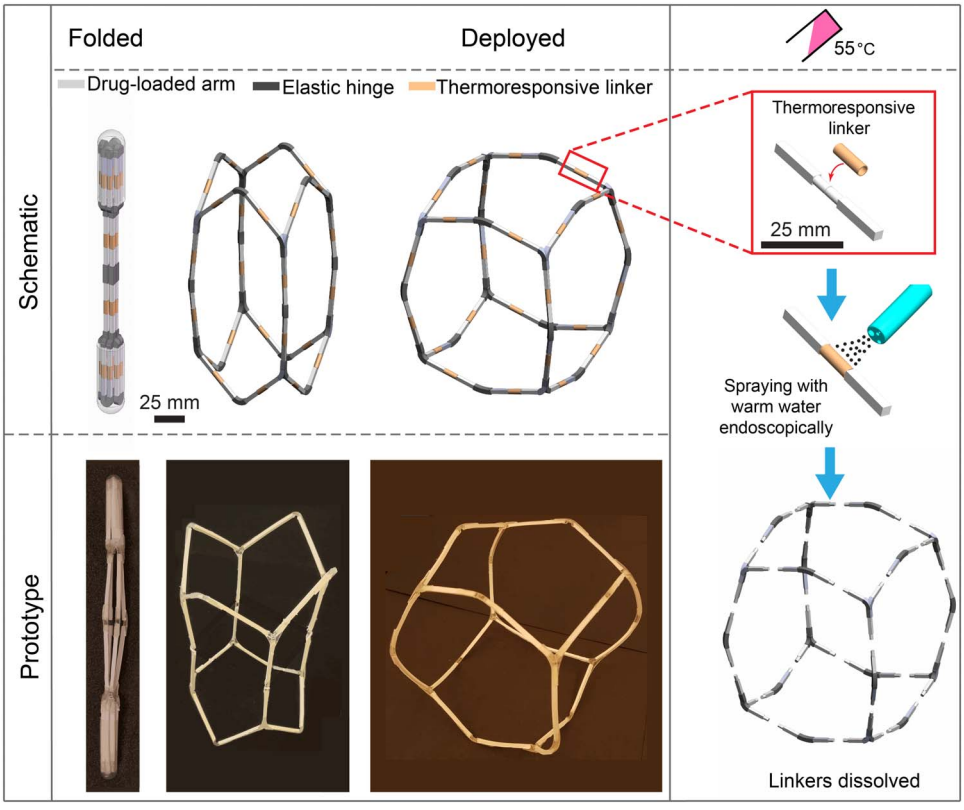

Fig. 4. Flexible mechanical metamaterial as a macrostructure dosage form. The schematic and prototype images of the metamaterial dosage form illustrating the sequence of deployment in stomach and the building components including drug-carrying arms (light gray), elastic hinges (dark gray), and TRLs (orange). The right panel shows temperature-triggered configuration by endoscopically applying warm water (55°C) to trigger the disassembly.

stomach and pass through the intestine without potential obstruction or perforation.

In vivo gastric residence and extended drug release

To evaluate the performance of the macrostructure dosage form for extended release, we loaded the dosage form with two drugs: (i) carbamazepine (CAR), a drug commonly used to treat epilepsy and bipolar disorder, and (ii) moxifloxacin (MOX), an antibiotic for treating bacterial infections. Poor adherence, estimated from 50 to 70%, is the major cause of treatment failure and poorly controlled epilepsy (*23*, *24*) and bacterial infections (*25*). The average daily dose for both drugs is between 200 and 400 mg (*26*, *27*), requiring high-capacity macrostructures for extended drug delivery. We confirmed the stability of both drugs in simulated gastric fluid (SGF) at 37°C, a prerequisite for use in our dosage form (fig. S9A). The drugs showed no degradation at elevated temperatures that may be reached during the manufacturing of the dosage form (fig. S9B).

We synthesized polymeric formulations for controlled release of the drugs and investigated in vitro drug release by varying drug loading, the composition of excipients, and the polymeric coating (fig. S9, C and D). To achieve long-term gastric residence, drug-loaded arms with different formulations must retain sufficient mechanical strength to withstand gastric contractions. A comprehensive mechanical characterization of drug-polymer arms in SGF using a three-point bending assay was conducted (fig. S10). Note that the drug-polymer arms needed to be flexible enough over time to endure gastric forces and avoid breaking. The mechanical strength of the interfaces between drug-loaded arms and elastic hinges was assessed using uniaxial tensile tests on devices incubated in SGF, before and after exposure to warm water (55°C water); these tests revealed that temperature had a negligible effect on bonding (fig. S11).

Having identified the optimal formulations for extended drug release and mechanical strength and flexibility, MOX and CAR formulations (Fig. 3A) were selected to manufacture the macrostructure with the capacity to carry ~3 g of drugs, providing a daily dose of 215 mg for over 2 weeks. The optimal formulations exhibited linear drug release up to 25% over 14 days, as well as an ultimate flexural strength of >8 MPa and ultimate flexural strain of >0.08 even after 14 days of incubation in SGF at 37°C (Fig. 5A). Radiographic and endoscopic evaluation of the gastric residence of the macrostructure (Fig. 5B) revealed that, when deployed in the stomach, the macrostructure adopted a semispherical shape and was retained for 2 weeks without any fracture or disassembly. No evidence of GI obstruction, ulceration, or injury was observed. The gastric residence and in vivo drug release experiments were performed with dosage forms that did not contain TRLs for safety evaluation.

The serum concentrations of CAR administered using the macrostructure are reported in Fig. 5C. In animals treated with the immediate release formulations, drug was detected until 1 day post dose. In one of the animals, we did observe drug concentrations on day 6 and 8, which may be related to the slow gastrointestinal transit time in pigs. In contrast, the macrostructure delivered drug consistently for 14 days. The macrostructure also allowed a tempered maximum serum concentration, denoted by C_{max}, and enhanced area under the curve, denoted by AUC, attributable to the sustained release of the drug (Fig. 5D).

We synthesized TRLs that retained mechanical stability in SGF and rapidly weakened upon spraying with 55°C water. Mechanical stability and thermal response of the drug-loaded arms with TRLs were evaluated using a three-point bending test (Fig. 5E). A significant reduction ($^*P < 0.05$) in average ultimate flexural strength (8 to 1.5 MPa) and ultimate flexural strain (0.06 to 0.02) was observed over 14 days when devices were triggered with 55°C water. These data were confirmed by endoscopically triggering the macrostructure TRLs in vivo (Fig. 5F).

DISCUSSION

Here, we describe the development of esophageal and gastric-resident drug delivery systems. We developed two prototype devices that exhibited tunable temperature-responsive material properties and controllable dissolution: a flower-like device for deployment in the esophagus

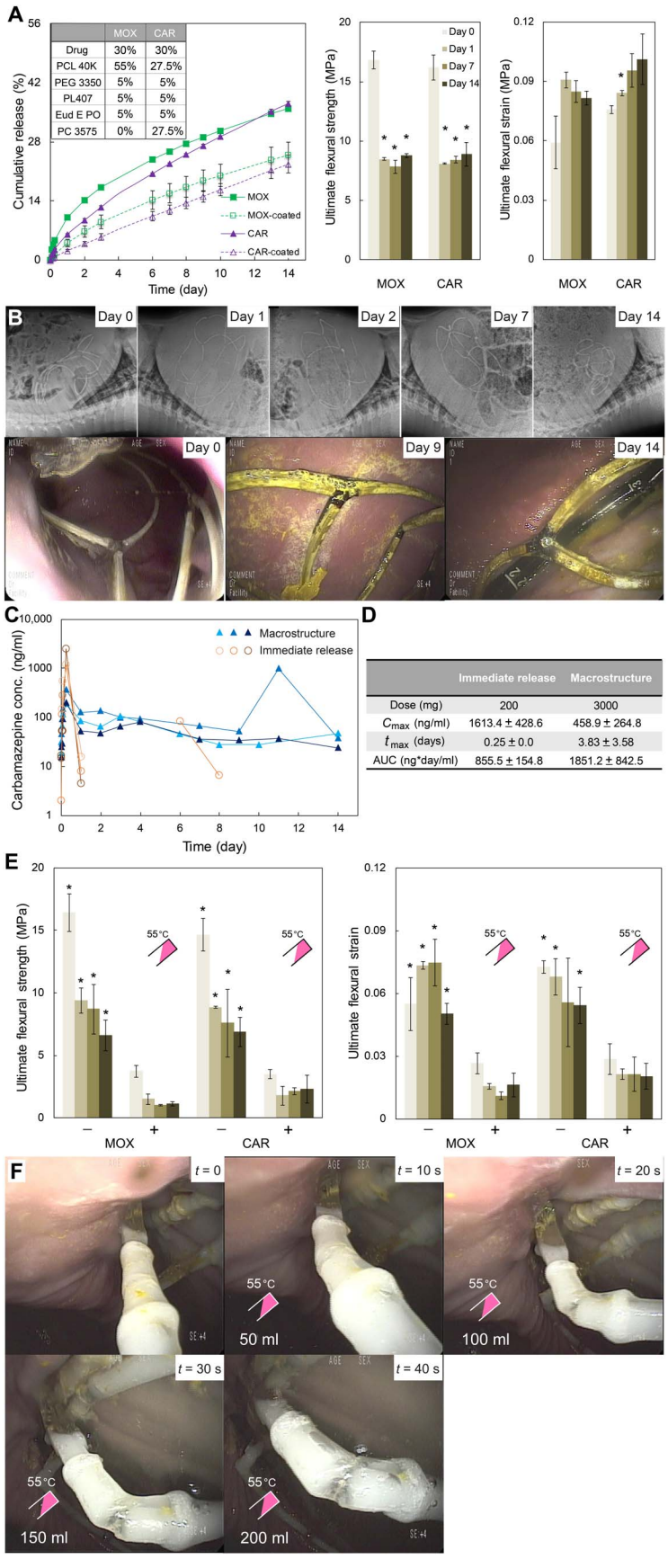

Fig. 5. Characterization of metamaterial dosage form in vitro and in vivo. (**A**) In vitro cumulative drug release and ultimate flexural strength and strain of drug-loaded arms for MOX and CAR formulations incubated in 37°C SGF for 14 days. Markers and column bars represent the mean ± SD for $n = 3$ samples per group. *$P < 0.05$, one-way ANOVA and post hoc Bonferroni multiple comparison tests were used to determine the significance (days 1, 7, and 14 versus day 0). (**B**) Representative abdominal radiographs and endoscopic images obtained at various time points after metamaterial dosage form administration. (**C**) Serum concentration profiles over 15 days and (**D**) pharmacokinetic analysis of CAR administered as an immediate release formulation (orange) versus macrostructure dosage form (blue). (**E**) Effect of temperature on ultimate flexural strength and strain of drug-loaded arm segments with TRLs incubated in 37°C SGF for 14 days. Two-sample *t* tests were used to determine the significance. *$P < 0.05$ [not exposed to warm water (–) versus exposed to warm water (+)]. (**F**) In vivo endoscopic images showing the weakening sequence of a TRL for a macrostructure after spraying 200 ml of 55°C water 7 days after gastric metamaterial dosage form deployment in a porcine model.

and a metamaterial dosage form for long-term gastric residence. Devices that currently transiently reside in the esophagus (including those devices that inadvertently reside there because of errors during deployment) require endoscopic retrieval. The ability to impart esophageal delivery systems with temperature-sensitive means to change shape and pass into the gastric cavity amplifies our capacity to develop therapeutic modalities with greater safety profiles and functionality.

Over the past decade, we have witnessed considerable growth in GI device development; however, device removal remains limited to endoscopy, which can be associated with significant morbidity during gastric and esophageal endoscopic extraction leading to tissue perforation (*16*). The ability to apply metamaterial principles, combined with our understanding of temperature-triggered materials, helps establish a route toward potentially safer in situ device disintegration in the GI tract with subsequent excretion of the smaller individual segments.

Here, we describe the fundamentals of heat dissipation in the upper GI tract of a large animal model via administration of a warm fluid. Successful translation into human application will require the study and evaluation of heat dissipation across a range of human subjects varying in their dimension to inform optimal boundary conditions. Furthermore, our work has focused on using liquids for triggering, and further study of warm solids is likely warranted to inform optimal and safe temperature boundaries in the upper GI tract. We anticipate the potential for targeted temperature-inducing or transferring interactions using ingestible systems homing to a device, through, for example, the use of magnets, as well as the application induction or remote triggering of a heat-producing reaction.

Our findings of heat dissipation throughout the upper GI tract and temperature-triggerable metamaterials provide a new approach for developing GI technologies with fast and robust responses. Combining design principles of transformable architected materials and thermoresponsive elements offers a unique drug delivery mechanism with a range of advantages. The proposed esophageal flower-inspired prototype can rapidly reconfigure by ingestion of warm fluid, and the flexible macrodevice can be safely retained within the stomach until warm fluid is applied endoscopically to trigger the disassembly and excretion of device components. Although we focused on

extended high-capacity drug delivery application of the macrodevice, other potential clinical applications are anticipated, including nutritional modulation for bariatrics and obesity treatment, as well as ingestible electronics for diagnosis and sensing. Our data provide insight into temperatures within the GI tract, which could be used to trigger response in materials and characterize the heat dissipation via ingestion of warm fluid as a function of multiple drinking volume rates. We expect that our results will serve as a guide for the design of temperature-responsive drug delivery systems with a wide range of applications for deployment in the GI tract.

MATERIALS AND METHODS

Study design

The goal of this study was to develop temperature-triggerable devices for GI applications with robust and ultrafast response. This objective was addressed by (i) characterization of warm water heat dissipation in the upper GI tract of a large animal model and determining temperature-triggerable regions through ingestion of warm water and (ii) developing a temperature-triggerable esophageal system for potential stenting and drug delivery applications, as well as the control of macrodevices for extended drug release in the extra-esophageal compartments in a large animal model. All animal experiments were conducted in accordance with protocols approved by the Committee on Animal Care at the Massachusetts Institute of Technology (MIT). All the in vivo tests have been performed in a large animal model (50- to 80-kg Yorkshire pigs ranging between 4 and 6 months of age). The pigs were provided by the Cummings School of Veterinary Medicine at Tufts University. The pig was chosen as a model because its gastric anatomy is similar to that of humans and has been widely used in the evaluation of biomedical GI devices (*28*, *29*). After overnight fasting, the animals were sedated with TELAZOL [tiletamine/zolazepam; 5 mg/kg, intramuscular (IM)], xylazine (2 mg/kg, IM), and atropine (0.04 mg/kg, IM) followed by endotracheal intubation and maintenance anesthesia with inhaled isoflurane (1 to 3% in oxygen). For extended release study, animals were monitored clinically at least twice a day for any evidence of morbidity, including lethargy, inappetence, decreased fecal output, abdominal distension, and vomiting. No adverse events, obstruction of pylorus, or limitation in passage of food or liquid was observed during the studies associated with these dosage forms. Endoscopic evaluation of the stomach over the course of the study was performed to further explore the stomach and ensure the absence of any ulceration or injury. Blood samples were taken from peripheral veins under sedation at the following time points: 0 min (before administration of the dosage form), 5 min, 15 min, 30 min, 2 hours, and 6 hours, daily for a minimum of 5 days and then three times for the second week. Group and sample size for each experiment are indicated in each figure legend. Primary data are reported in data file S1.

In vivo temperature testing

The temperature in the esophagus and stomach during administration of warm water was measured in a large animal model (three Yorkshire pigs). After anesthesia, an endoscopic overtube (US Endoscopy) was placed into the esophagus under endoscopic visual guidance during esophageal intubation. Next, the temperature setup, made of an array of 16 thermocouple probes, was inserted through the overtube into the esophagus and stomach, and the overtube was then removed. When the correct placement was confirmed by radiographs (the position of all the probes was matched across all the experiments), the overtube was withdrawn such that the distal tip was at the proximal esophagus. Then, the pigs were secured in the seated position to mimic the orientation of the human GI tract while drinking.

A temperature measurement setup was fabricated to monitor temperature changes in the GI tract during the administration of a warm liquid. The setup was composed of an array of 16 bead wire K-type thermocouple probes (model number: TP8735M, Extech Instruments) attached together using waterproof vinyl tape (part number: 190T, 3M) with 5-cm spacing between each thermocouple (shown in fig. S1). The thermocouple probes have a wide operating temperature range from −30° to 300°C with an accuracy of ±1°C and a 5-m-long bead wire, enabling precise temperature measurement in narrow orifices of the digestive system such as the esophagus. The temperature data were recorded using a data logger (four-channel K-type thermometer with SD card data; model number: 88598, AZ Instruments) with a resolution of 0.1°C, allowing real-time monitoring of the luminal temperature. A total of four four-channel data loggers were used to record data from 16 thermocouple probes. The setup was initially evaluated in vitro by inserting it into a 40-cm-long Tygon tubing with the same inner diameter as the esophagus (~18 mm). Temperatures were recorded after administration of water at different volumetric flow rates and input temperatures. The data obtained experimentally confirmed that the setup had perfect accuracy and repeatability (fig. S2A).

A range of volumes of 55°C warm water (V = 10, 20, 50, 100, 200, and 250 ml) were administered in 10 s (steady-state flow rate), and the temperature was recorded using the data loggers for all the probes. In fig. S2B, we reported the variation of temperature for probe numbers n = 1, 2, 3, and 4 positioned in the esophagus. Upon administering 100 ml of 55°C water, the temperature considerably rose from the body temperature (~ 35°C) to 47 ° to 49°C, which is lower than the 55°C ingested water because of heat dissipation in the esophagus. Each measurement was repeated three times in three different pigs with 2-min intervals between the tests to ensure that the body temperature recovered to its initial value (35 ° to 37°C) before beginning a new test. For the high volumes of input water (V = 100, 200, and 250 ml), we evacuated the water in the stomach using vacuum suction after every measurement. The pouring period was 10 s for all the volumes except for V = 10 and 20 ml, where we poured the entire volume of water quickly to mimic a single gulp. Last, we calculated the change in the upper GI tract temperature (ΔT), defined as $\Delta T = T_i - T_{\text{Body}}$ where T_i denotes the temperature measured by the probe number i, i = 1, 2, …, 16, and T_{Body} denotes the body temperature, which varies between 35 ° and 37°C.

Flower-like prototype manufacturing

The flower-like prototype is a multimaterial design manufactured from three materials: (i) a thermoplastic polyester, PCL (molecular weight, 40 kDa; Capa 6400, Perstorp), used for the arms and central core; (ii) a thermoplastic polyurethane, Elastollan 1185A (BASF), used for the L-beam–shaped elastic recoil element; and (iii) shape-memory nitinol (NiTi) with a nominal transition temperature of 50°C for torsion springs (Nexmetal Inc.) (all shown in fig. S3). Two aluminum molds were fabricated using a Computer Numerical Control (CNC) mill (Othermill Pro, Bantam Tools) to cast the PCL arms and Elastollan 1185A recoil elements (L-beam shaped) via a two-step compression molding process. First, Elastollan 1185A pellets were melted in the L-beam mold in an oven at 250°C for 10 min (fig. S4A). After compression and demolding, the flash was removed from the newly cast L-beams using a razor blade. Second, the L-beams were placed in the

arm mold (fig. S4B), and PCL pellets were melted using a heat gun at 175°C (sufficient to melt PCL but not Elastollan 1185A). The L-beam recoil elements and PCL were compressed using a weight that forced the PCL around the ends of the elements and created a robust junction (fig. S4C). A silicone rubber mold (Elite Double 32, Zhermack SpA) was used to cast the PCL central core (fig. S4D). First, the core was fabricated using a 3D printer (Objet30 Pro, Stratasys) with VeroBlue (product number: RGD840, Objet) plastic material. Then, the negative mold was cast using the silicone. Last, the PCL core was cast by melting PCL pellets in the silicone mold using a heat gun at 175°C followed by compression molding. After demolding and removing the flash, four 10-mm-deep holes were drilled into the bottom of the core using a 0.60-mm drill bit. The holes were located at the midpoints of each edge of the bottom face's square cross section (fig. S4E). To assemble the prototype, one end of each torsional spring was glued to the outside of each arm using a strong adhesive (Krazy Glue). After drying, glue was brushed onto the other ends of the nitinol torsion springs, which were lastly inserted into the corresponding holes in the core (fig. S4F).

Nitinol heat treatment

The shape-memory nitinol was set using a fixture designed to hold it in the shape of the desired torsion spring inside a high-temperature laboratory oven (LHT 6/30, Carbolite Gero), as shown in fig. S5. The fixed nitinol wire was placed inside the preheated oven at 500°C for 20 min and quenched in a room temperature water bath. The ends of the torsion spring are cut down to 10 mm each using a wire cutter. This ensures that the maximum dimension of the spring is no more than 20 mm and sufficient to pass through the pylorus.

Mechanical characterization of the flower-like prototype

To ensure that the flower-like prototype is capable of robust (i) deployment (opening) due to elasticity of the central elastic recoil elements (Elastollan 1185A) and (ii) closure (folding) in response to thermal triggering of the nitinol springs, the recoiling forces of the elastic recoil elements and shape-memory nitinol springs, denoted by $F_{cr}^{Elastollan}$ and $F_{cr}^{nitinol}$, respectively, were experimentally measured. To measure the elastic recoiling force, $F_{cr}^{Elastollan}$, the prototype was fixed to the bottom of a uniaxial testing machine (Instron 5942 Series Universal Testing System) with a 10-N load cell. In this configuration, three of four arms were folded and one was free to move (fig. S6A). The free arm was then pushed directly down by the tester until fully folded. The peak load was recorded as the recoiling force, which is the same as the force exerted from each arm upon expansion of the prototype. For the selected dimensions of the Elastollan L-beam recoil element, which were chosen because of manufacturing limitations, $F_{cr}^{Elastollan} = 0.4$ N was recorded.

To measure the springs' recoiling force $F_{cr}^{nitinol}$, in response to a temperature change, a 50-N force gauge (FG-3005, Shimpo Instruments) with a hook attachment was clamped in a retort stand. One arm of nitinol springs with nominal transition temperature $T_c = 50$°C and variable coil numbers and diameters was fixed, and the other arm interfaced snugly with the hook. Warm water at 50°C was poured onto each spring with differing number of coils and coil diameters, and the peak load recorded by the force gauge was taken as the spring recoiling force (fig. S6B).

In vivo testing of the flower-like prototype

Three female Yorkshire pigs were used for in vivo evaluation. After overnight fasting, the animals were sedated. An overtube (US Endoscopy), with endoscopic guidance, was placed into the proximal esophagus to assist the placement of the flower-like prototype while being held in folded (closed) configuration by a single-use endoscopy snare (Captivator II, Boston Scientific). Once in position, 100 ml of 55°C water was administered via the overtube into the esophagus to thermally trigger the nitinol springs. This resulted in fully folding the prototype. The prototype was then allowed to pass into the pig's stomach, where it was retrieved intact. The same experiment was performed with the prototype in the reverse direction. The details of deployment, closure, and passage of the flower-like prototype for both direct and reverse directions were recorded and presented in movies S1 and S2, respectively. After the above procedures, the animals were recovered and were monitored clinically at least twice a day for any evidence of morbidity, including lethargy, inappetence, decreased fecal output, or any other abnormal signs.

Degradable polymeric millineedle manufacturing

The millineedles were fabricated from a mixture of Soluplus (BASF) and ethanol (EtOH), with the addition of 70-kDa dextran labeled with Texas Red (Thermo Fisher Scientific) or budesonide (Carbosynth) at different points in the fabrication process. To manufacture the polymeric degradable needles, a molding approach was used. First, negative silicone molds were fabricated by casting a silicone rubber (Elite Double 32, Zhermack SpA) using metal 3D printed needles (designed in-house, printed by Protolabs; shown in fig. S7A). Then, the needles were cast into the silicone molds using a [1:1 (w/w)] polymeric mixture of ethanol and Soluplus (fig. S7B). For x-ray visualization, 15% (w/w) of $BaSO_4$ was added to the polymeric mixture.

To enable fluorescence imaging, Texas Red–labeled dextran was loaded into the millineedles. To prepare these millineedles, a solution (25 mg/ml) of Texas Red–labeled dextran in EtOH was prepared, and then, 20 μl of this solution was added to the Soluplus/EtOH mixture. The mixture was mixed using a DAC 150.1 FVZ-K SpeedMixer (FlackTek Inc.) for 5 min at about 3000 rpm to create a homogeneous solution. The silicone molds were filled with the polymeric solution.

To make millineedles loaded with budesonide, 1 μl of a suspension (100 mg/ml) of budesonide in EtOH was pipetted into the tips of the silicone molds before pouring the polymeric solution, ensuring to mix the suspension during pipetting. This resulted in 0.1 mg of budesonide loaded at the tips of needles. The molds were then placed in a evaporation system (GeneVac DD-4X) to spin-cast at room temperature and left for 3 days for EtOH to evaporate completely. The millineedles were then demolded, and the substrates were sanded down to a thickness of about 1 mm and trimmed down to fit on the tips of the flower-like prototype's arms using a razor blade. The millineedles were lastly mounted to the arms using an adhesive (Krazy Glue).

Ex vivo testing of the flower-like prototype

Macromolecule delivery

The flower-like prototype with three needles loaded with dextran labeled with Texas Red and one control needle loaded with only dextran (no Texas Red) was deployed in the esophagus harvested from a Yorkshire pig 10 min after euthanasia. The method of euthanasia complies with the American Veterinary Medical Association (AVMA) Guidelines on Euthanasia (*30*) and was approved in the MIT Committee on Animal Care protocol. Pigs are anesthetized before euthanasia with an intravenous administration of sodium pentobarbital (~100 mg/kg). The esophagus was rinsed for about 10 s under running tap water to

wash away contaminants such as gastric fluid. To deploy the prototype, a custom 3D printed fixture was used. The fixture consisted of a 10-mm square tube 3D printed (Formlabs, Form 2) out of rigid plastic (product number: RS-F2-GPGR-04, Formlabs) and a 20-mm-diameter tube 3D printed (Objet30 Pro, Stratasys) out of VeroClear plastic (product number: RGD810, Objet). The 20-mm tube was placed inside the ex vivo esophagus to hold it open for deployment, and the prototype was placed inside the square tube. The prototype and the square tube were then inserted into the esophagus via the 20-mm tube. Once it reached the mid-esophagus, the prototype was pushed out of the square tube to deploy. After deployment, the prototype was left in place for 20 min before retrieval. The Texas Red deposition was assessed using an IVIS Spectrum In Vivo Imaging System (PerkinElmer) at a fluorescent excitation and an emission filter set to 570 and 620 nm, respectively.

Histological analysis was performed on tissue biopsies to characterize the depth of penetration. Biopsies were taken at the penetration sites, where needles coated with green tissue marking dye (product number: 0736-3, Cancer Diagnostics Inc.) penetrated. The biopsies were fixed in formalin fixative (Sigma-Aldrich) for 24 hours before transfer to 70% ethanol. Tissue samples were then embedded in paraffin, cut into 5-μm-thick tissue sections, and imaged using an Aperio AT2 Slide Scanner (Leica Biosystems).

Small-molecule delivery

Three flower-like prototypes, each equipped with three needles loaded with 0.1 mg of budesonide per needle and one control needle, were deployed in the esophagi of three Yorkshire pigs (esophagi harvested 10 min after euthanasia). Needles were maintained within the esophagus for 20 min to allow for degradation before retrieving the esophagus, taking 8-mm-diameter biopsies at the four needle penetration sites. The biopsies were frozen until extraction. Budesonide was extracted from the tissue by placing each biopsy in methanol and shaking at 100 rpm in room temperature overnight. The samples were centrifuged at 1500*g* for 10 min, and a fraction of the supernatant was collected. These samples were evaporated to dryness, spiked with 200 μl of hydrocortisone (250 ng/ml; internal standard) in acetonitrile to cause precipitation of any remaining proteins. Samples were vortexed and sonicated for 10 min and centrifuged for 10 min. Two hundred microliters of supernatant were pipetted into a 96-well plate containing 200 μl of Nanopure water and used for ultraperformance liquid chromatography–tandem mass spectrometry (UPLC-MS/MS) analysis.

UPLC-MS/MS analysis of small-molecule delivery through millineedles

UPLC-MS/MS analysis was performed on a Waters ACQUITY UPLC I-Class System aligned with a Waters Xevo TQ-S mass spectrometer (Waters Corp.). Liquid chromatographic separation was performed on an ACQUITY UPLC Charged Surface Hybrid C18 (50 mm × 2.1 mm, 1.7-μm particle size) column at 50°C. The mobile phase consisted of aqueous 0.1% formic acid and 10 mM ammonium formate solution (mobile phase A) and an acetonitrile: 10 mM ammonium formate and 0.1% formic acid solution [95:5 (v/v)] (mobile phase B). The mobile phase had a continuous flow rate of 0.6 ml/min using a time and solvent gradient composition. The initial composition (100% mobile phase A) was held for 1 min, after which the composition was changed linearly to 50% mobile phase A over the next 0.25 min. At 1.5 min, the composition was 20% mobile phase A, and at 2.5 min, the composition was 0% mobile phase A, which was held constant until 3 min. The composition returned to 100% mobile phase A at 3.25 min and was held at this composition until completion of the run, ending at 4 min, where it remained for column equilibration. The total run time was 4 min, and sample injection volume was 2.5 μl. The mass spectrometer was operated in the multiple reaction monitoring (MRM) mode. Sample introduction and ionization was by electrospray ionization (ESI) in the positive ionization mode. MassLynx 4.1 software was used for data acquisition and analysis.

Stock solutions of budesonide and internal standard hydrocortisone were prepared in methanol at a concentration of 500 μg/ml. A 12-point calibration curve was prepared in methanol ranging from 1 to 5000 ng/ml.

Flexible metamaterial (macrostructure dosage form) manufacturing

The macrostructure dosage form was fabricated from three constitutive materials: (i) PCL (molecular weight, 40 kDa; Capa 6400, Perstorp), used for the arms; (ii) Elastollan 1185A (BASF), used for the elastomeric joints; and (iii) TRLs made from a 1:2 (w/w) mixture of low–molecular weight PCL (molecular weight, 10 kDa; Sigma-Aldrich) and polycarbonate-based thermoplastic polyurethane (PC-3575A, Lubrizol). Depending on the drug used, the arms have excipients and elasticizers added to enhance the drug release and mechanical properties, respectively. For both MOX (Alchem Pharmtech Inc) and CAR (Ark Pharm Inc), poly(ethylene glycol) (PEG) (molecular weight, 3350 Da; Spectrum Corp.), Kolliphor P 407 (BASF), and EUDRAGIT E PO (Evonik Industries) were used as excipients; for CAR, Carbothane thermoplastic polyurethane (TPU) PC3575A was used as an elasticizer. For x-ray visualization, 15% (w/w) of $BaSO_4$ was added. The Computer-Aided Design (CAD) model of the metamaterial dosage form is presented in fig. S8.

Drug-loaded arms with various formulations were synthesized by mixing the materials in a microcompounder (Xplore MC 5) at 120°C and then by injection molding of the hot melt using an injection molding machine (Xplore IM 5.5). The arm molds were designed to fabricate two arms at a time, but the pressure profile for each drug formulation was different because of differing viscosities in their molten phase. For MOX, the pressure profile was an initial pressure of 0.5 bar for 1.0 s, ramp to 0.7 bar in 1.0 s, and a sustained pressure of 0.7 bar for up to 3.0 s. For CAR, the pressure profile was an initial pressure of 1.0 bar for 2.0 s, ramp to 1.5 bar in 2.0 s, and a sustained pressure of 1.5 bar for up to 8.0 s. To join the arms, Elastollan 1185A was melted in the same microcompounder at a uniform temperature of 225°C and extruded into molds with the arms for compression molding. First, the corners made up of three arms were cast in a two-part mold with a silicone bottom to hold the arms in place and an aluminum top, which was CNC-milled and used to compress the Elastollan 1185A melt. The silicone mold was fabricated by the same method described in earlier sections. The corners were then joined in pairs using similar molds to assemble the top and bottom faces. Last, the top and bottom faces were joined, although only one silicone mold and a weight instead of a top mold were used to compress the Elastollan 1185A melt.

The arms were dip-coated using a solution of 5.4% (w/v) PCL and 0.6% (w/v) EUDRAGIT E PO in acetone. The solution was then left to stir at 200 rpm on a 50°C hot plate for 20 min until the homogeneous solution appeared. Each arm was submerged in the solution for about 1 s and then left to dry in a fume hood. This was repeated five times per arm to produce a consistent and homogeneous coating.

Drug stability assessment

Given that the macrostructure cube dosage form is designed to reside in the stomach for an extended period, we analyzed drug stability in

SGF [0.2% (w/v) sodium chloride and 0.7% (w/v) hydrochloric acid, adjusted to pH 1.2]. MOX was dissolved in SGF and placed at 37°C. At various times, part of the solution was aliquoted and stored at −20°C until further analysis. For CAR, the drug was first dissolved in methanol and then diluted in SGF (at least 100-fold). At various times, part of the solution was collected and stored at −20°C. On completion of the study, drug concentration in the various aliquots was measured using high-performance liquid chromatography–ultraviolet (HPLC-UV) analysis described in the "HPLC-UV analysis of drug release" section.

CAR is stable in SGF for the duration of the experiment (fig. S9A). In addition, we measured drug stability at elevated temperatures that may be reached during the manufacturing of the dosage form. In these studies, no appreciable drug degradation was observed (fig. S9B).

HPLC-UV analysis of drug release

HPLC was performed using a 1260 Infinity System (Agilent Technologies Inc.), equipped with a 1260 quaternary pump, a 1260 Hip ALS autosampler, a 1290 thermostat, a 1260 TCC control module, and a 1260 diode array detector. Data acquisition was monitored and processed using a ChemStation software (Agilent Technologies Inc.). For both drugs, MOX and CAR, chromatographic separation was carried on a Poroshell 120 EC-C18 column (4.6 mm by 50 mm, 2.7 μm) column (Agilent Technologies Inc.). For CAR, an isocratic method, which was 50% water and 50% methanol (v/v), was used. The injection volume was 5 μl. The column was maintained at 40°C, and the flow rate was 1 ml/min. The total run time was 5 min. Absorbance was measured at 285 nm. For MOX, a biphasic gradient method was used. Mobile phase A was a potassium dihydrogen orthophosphate buffer (pH 3), and mobile phase B was acetonitrile. At 0 min, the composition was 100% mobile phase A. The composition was changed linearly to 0% mobile phase A until 2.5 min where it was held until the end of the run at 5 min. The post time was 3 min to allow for column equilibration. The injection volume was 5 μl. The column was maintained at 50°C, and the flow rate was 1 ml/min. Absorbance was measured at 293 nm.

In vitro release from drug-loaded arms in SGF

We synthesized various polymeric formulations of CAR and MOX and studied the effect of changing drug loading, nature, and composition of additives and application of polymeric coating on drug release. The summary of the different formulations used for in vitro release from drug-loaded arms in SGF is listed in fig. S9C. Because of the limited solubility of CAR in SGF, 5% (w/v) Tween 20 was added to the release medium. To perform the release study, drug-polymer matrices (~1 cm in length) were incubated with 50 ml of the respective release medium in a 37°C incubator shaker at 50 rpm. At various times, 1 ml of the release medium was collected and stored at −20°C until further analysis. The remaining medium was discarded, and the arms were incubated with fresh medium. For measuring drug concentrations in the release medium, all specimens (beam-like arms) were thawed, centrifuged at 1500*g* for 10 min, and analyzed using HPLC.

The rate and extent of drug release could be tuned by optimal configuration of these factors. For example, the fraction of MOX released over 2 weeks doubled (and total amount of MOX release nearly tripled) upon increasing MOX loading from 35% (w/w) to 50% (w/w) (compare MOX-01 to MOX-03; fig. S9D). Drug release could be accelerated further by the inclusion of a surfactant such as Pluronic P407 (MOX-04; fig. S9D). Inclusion of hydrophilic excipients had similar effects on the release of CAR. Release of CAR increased by >3-fold by the addition of water soluble polymers such as PEG 3350 and Kolliphor P 407 to the polymer matrix (compare CAR-01 and CAR-03; fig. S9D). This increase in drug release could be attributed to a higher initial burst and an overall increase in the rate of drug release during the zero-order phase. The initial burst could be suppressed by coating the polymer matrix with a thin layer of PCL and EUDRAGIT E PO (compare CAR-03 and CAR-03–coated; fig. S9D). In summary, we identified a range of formulations of MOX and CAR where the release could be modified to achieve the desirable pharmacokinetics.

Mechanical characterization of drug-loaded arms

To achieve long-term gastric residence, drug-loaded arms with different formulations must retain sufficient mechanical strength and flexibility (ductility) to withstand gastric contractions, particularly after most of the drug is released over time. The effect of SGF on the mechanical performance of different formulations was characterized using a three-point bending assay (ASTM D790-17 standard). The specimens (drug-loaded arms) were placed in 50 ml of SGF and left for 1, 7, and 14 days in a 37°C incubator shaker at 100 rpm. The bending test was then conducted for each time point and a day 0 control. The data are reported in fig. S10A (ultimate flexural strength) and fig. S10B (corresponding flexural strain) for both drugs across various formulations, showing an ultimate flexural strength of >10 MPa and an ultimate flexural strain of >0.06 (except CAR-01) even after 14 days in SGF for all the formulations. To improve the flexibility of the drug-polymer arms, we included an elasticizer, polycarbonate-based thermoplastic polyurethane (PC-3575A, Lubrizol), to the formulations (CAR-02, CAR-03, and CAR-04). CAR-01 is an example of a relatively brittle formulation (ultimate flexural strain ~ 0.012 with no elasticizer included) that readily fractured into small pieces in stomach after delivery, even showing high strength (an ultimate flexural strength of >35 MPa). MOX formulations naturally exhibited a ductile response (an ultimate flexural strain of >0.06) that guaranteed high durability of the drug-polymer arms for prolong gastric retention.

Three-point bending test of drug-loaded arms

Three-point bending tests on the various drug-loaded arms were conducted according to ASTM standard D790-17. A uniaxial testing machine (Instron 5942 Series Universal Testing System) with a 500-N load cell equipped with a three-point bending fixture was used to test specimens. The specimens were beam-like arms with a square cross section (side length, 2.6 mm; length, 55 mm). The support span was set to 41 mm, in accordance with the ASTM standard [16:1 ratio of span to thickness (of specimen) shall be used]. The required rate of crosshead motion R was calculated to be 1.1 mm/s by the equation $R = zl^2/6d$, where z is the outer fiber strain rate fixed at 0.01, $l = 41$ mm is the support span, and $d = 2.6$ mm is the specimen thickness. However, to facilitate rapid testing, the rate of crosshead motion was set to 4.4 mm/s (four times faster) with no effect on the bending response. The force-displacement curves were recorded. The data were then converted to engineering flexural stress, $\sigma_f = 3fl/2b^3$, as a function of engineering flexural strain, $\epsilon_f = 6ud/L^2$, where f and u are the displacement and force at the center of the specimens. Last, the ultimate flexural strength (denoted by σ_f^U) and corresponding flexural strain (denoted by ϵ_f^U) were calculated using $\sigma_f^U = 3f^{max}l/2b^3$ and $\epsilon_f^U = \epsilon_f$ at $\sigma = \sigma_f^U$, respectively, where f^{max} is the peak force.

To assess the effect of SGF on the mechanical properties of different formulations, the specimens were placed in 50 ml of SGF and left for 1, 7, and 14 days in a 37°C incubator shaker at 100 rpm. The aforementioned three-point bending test was then conducted for each time point, as well as a day 0 control. The same test was performed for the drug-loaded arms connected with TRLs, considering additional specimens for bending with and without the presence of 55°C warm water. These tests were performed while the thermal linkers were immersed in the warm water.

Uniaxial tension test of drug-loaded arms

To determine the effect of gastric fluid on the bond strength between the elastomeric Elastollan elements and the drug-polymer arms, a uniaxial tensile test was conducted on specimens 110 mm in length with a square cross section (side length, 2.6 mm). Half the length of each specimen (55 mm) was made of Elastollan 1185A, and the remaining half was synthesized from a given formulation for the arms (PCL, MOX, and CAR). The two halves were joined by compression molding. To run the test, each end of the specimen was held in place using a pneumatic grip and pulled at a steady state at 1 mm/s, outputting plot of force against extension. Similar to the three-point bending tests, the specimens were placed in 50 ml of SGF for 1, 7, and 14 days and left in a 37°C incubator shaker at 100 rpm. The tensile test was then conducted for each time point and as a day 0 control. The effect of temperature was also investigated with an additional set of specimens that were submerged in 55°C water for 20 s before starting the test.

Mechanical performance of interfaces between the polymeric arms and elastic hinges

The structural integrity of the macrostructure dosage form in the stomach also depends on the interface between the drug-polymer arms and elastic hinges. We determined the strength of the interface between the PCL/selected drug-loaded arms and Elastollan 1185A recoil elastic hinges (PCL–ELS, Mox-04–ELS, and CAR-03–ELS), placed in 50 ml of SGF and left for 1, 7, and 14 days in a 37°C incubator shaker at 100 rpm. As explained in "Uniaxial tension test of drug-loaded arms" section, we performed uniaxial tensile tests to determine the ultimate tensile strength of the interfaces. The effect of temperature was also investigated with an additional set of specimens that were submerged in 55°C water for 20 s before starting the test. For both cases, minimal deterioration in the ultimate tensile strength was measured, as shown in fig. S11.

In vivo gastric retention and prolonged drug delivery of macrostructure dosage form

To evaluate the ability of macrostructure dosage forms, loaded with the selected CAR formulation, to achieve gastric retention, we administered them to a large animal model (three Yorkshire pigs for each drug). After overnight fasting and sedation of the animals, an overtube (US Endoscopy) was placed into the stomach with endoscopic guidance to facilitate direct gastric delivery of the macrostructure dosage forms. The folded macrostructures with a cylindrical shape (length, 20 cm; diameter, 12 mm) were administered via the overtube into the stomach, and the overtube was then removed. Serial radiographs were performed immediately and every 48 to 72 hours afterward to monitor the integrity and transit of the devices, as well as any radiographic evidence of bowel obstruction. Blood samples were obtained as explained in the "Study design" section.

Pharmacokinetics of drug delivered using macrostructure dosage form

One hundred microliters of each serum was spiked with 200 μl of internal standard (250 ng/ml; imipramine for CAR) in acetonitrile added to elicit protein precipitation. Samples were vortexed and sonicated for 10 min and centrifuged for 10 min at 13,000 rpm. Two hundred microliters of supernatant was pipetted into a 96-well plate containing 200 μl of Nanopure water. Last, 2.0 or 2.5 μl of the appropriate sample was injected onto the UPLC-ESI-MS system for analysis.

UPLC-ESI-MS analysis of in vivo drug release of macrostructure dosage form

CAR concentrations in serum were analyzed using UPLC-MS/MS. Analysis was performed on a Waters ACQUITY UPLC -I-Class System aligned with a Waters Xevo TQ-S mass spectrometer (Waters Corp.). Liquid chromatographic separation was performed on an ACQUITY UPLC Charged Surface Hybrid C18 (50 mm × 2.1 mm, 1.7-μm particle size) column at 50°C. The mobile phase consisted of aqueous 0.1% formic acid and 10 mM ammonium formate solution (mobile phase A) and an acetonitrile: 10 mM ammonium formate and 0.1% formic acid solution [95:5 (v/v)] (mobile phase B). The mobile phase had a continuous flow rate of 0.6 ml/min using a time and solvent gradient composition. The initial composition, 100% mobile phase A, was held for 1 min, after which the composition was changed linearly to 50% mobile phase A over the next 0.25 min. At 1.5 min, the composition was 20% mobile phase A, and at 2.5 min, the composition was 0% mobile phase A and 100% mobile phase B, which was held constant until 3 min. The composition returned to 100% mobile phase A at 3.25 min and was held at this composition until completion of the run, ending at 4 min, where it remained for column equilibration. The total run time was 4 min, and sample injection volume was 2.0 μl for CAR. The mass spectrometer was operated in the MRM mode. Sample introduction and ionization was by ESI in the positive ionization mode. MassLynx 4.1 software was used for data acquisition and analysis.

For the standard curve, stock solutions of CAR and their respective internal standards were prepared in methanol at a concentration of 500 μg/ml. A 12-point calibration curve ranging from 1 to 5000 ng/ml was prepared in blank serum for CAR.

Thermoresponsive linker

Similar to the solid arms, the two-part arm segments with the incorporated interlocking design were synthesized by mixing the materials in the microcompounder at 120°C and then by injection molding of the hot melt using the injection molding machine. The mold for each part was designed to fabricate one part at a time using the pressure with an initial pressure of 0.2 bar for 1.0 s, ramp to 0.5 bar in 1.0 s, and a sustained pressure of 0.5 bar for 3.0 s. To synthesize the thermal wraps, a mixture of 1:2 (w/w) of low–molecular weight PCL (molecular weight, 10 kDa; Sigma-Aldrich) and a thermoplastic polyurethane (PC-3575A, Lubrizol) was mixed in the microcompounder at a uniform temperature of 120°C and compression-molded into a bar shape. Using a preheated automatic film applicator (TQC), 300-μm flat films of thermosensitive linkers were fabricated. A CO_2 laser cutter (Universal Laser Systems) was then used to make 15 mm by 11 mm rectangular-shaped thin strips. Last, the polymeric thin films were wrapped around the two arm segments and connected using dichloromethane.

In vivo temperature triggering of macrostructure for disassembly

The macrostructure containing TRLs was deployed in the gastric cavity as described in the "In vivo temperature testing" and "In vivo gastric retention and prolonged drug delivery of macrostructure dosage form" sections. After 1 week of retention, the animal was fasted overnight. The gastric cavity was accessed endoscopically, and thermoresponsive linkages were sprayed with 200 ml of 55°C warm water. Serial endoscopic images were collected demonstrating disruption of the TRLs.

Statistical analysis

All the experimental data were reported as means ± SD for $n = 3$ measurements for each group. Two-sample t tests, one-way ANOVA, and post hoc Bonferroni multiple comparisons test were used to determine the significance.

SUPPLEMENTARY MATERIALS

stm.sciencemag.org/cgi/content/full/11/488/eaau8581/DC1
Fig. S1. Temperature testing setup.
Fig. S2. Evolution of temperature measured while administering warm water.
Fig. S3. Flower-like prototype.
Fig. S4. Fabrication and assembly of the flower-like prototype.
Fig. S5. Heat treatment of shape-memory nitinol.
Fig. S6. Mechanical characterization of the flower-like prototype.
Fig. S7. Fabrication of degradable millineedles.
Fig. S8. Reconfigurable mechanical metamaterial as a macrostructure dosage form.
Fig. S9. Drug stability and in vitro release of drug-loaded arms.
Fig. S10. Mechanical characterization of the drug-loaded arms by three-point bending tests.
Fig. S11. Mechanical characterization of the interfaces between the polymer arms and elastic hinges by uniaxial tension tests.
Movie S1. In vivo deployment, closure, and passage of the flower-like prototype in the esophagus.
Movie S2. In vivo deployment, closure, and passage of the flower-like prototype in the esophagus in the reverse direction.
Data file S1. Primary data (provided as an Excel file).

REFERENCES AND NOTES

1. S. J. R. Ellis, The distribution of bars at Pompeii: Archaeological, spatial and viewshed analyses. *J. Roman Archaeol.* **17**, 371–384 (2004).
2. F. Brown, K. R. Diller, Calculating the optimum temperature for serving hot beverages. *Burns* **34**, 648–654 (2008).
3. D. Loomis, K. Z. Guyton, Y. Gross, B. Lauby-Secretan, F. El Ghissassi, V. Bouvard, L. Benbrahim-Tallaa, N. Guha, H. Mattock, K. Straif; International Agency for Research on Cancer Monograph Working Group, Carcinogenicity of drinking coffee, mate, and very hot beverages. *Lancet Oncol.* **17**, 877–878 (2016).
4. H. S. Lee, M. O'Mahony, At what temperatures do consumers like to drink coffee?: Mixing methods. *J. Food Sci.* **67**, 2774–2777 (2002).
5. U. W. De Jong, N. E. Day, P. L. Mounier-Kuhn, J. P. Haguenauer, The relationship between the ingestion of hot coffee and intraoesophageal temperature. *Gut* **13**, 24–30 (1972).
6. Y.-W. Won, P. P. Adhikary, K. S. Lim, H. J. Kim, J. K. Kim, Y.-H. Kim, Oligopeptide complex for targeted non-viral gene delivery to adipocytes. *Nat. Mater.* **13**, 1157–1164 (2014).
7. A. R. Kirtane, O. Abouzid, D. Minahan, T. Bensel, A. L. Hill, C. Selinger, A. Bershteyn, M. Craig, S. S. Mo, H. Mazdiyasni, C. Cleveland, J. Rogner, Y.-A. L. Lee, L. Booth, F. Javid, S. J. Wu, T. Grant, A. M. Bellinger, B. Nikolic, A. Hayward, L. Wood, P. A. Eckhoff, M. A. Nowak, R. Langer, G. Traverso, Development of an oral once-weekly drug delivery system for HIV antiretroviral therapy. *Nat. Commun.* **9**, 2 (2018).
8. A. M. Bellinger, M. Jafari, T. M. Grant, S. Zhang, H. C. Slater, E. A. Wenger, S. Mo, Y.-A. L. Lee, H. Mazdiyasni, L. Kogan, R. Barman, C. Cleveland, L. Booth, T. Bensel, D. Minahan, H. M. Hurowitz, T. Tai, J. Daily, B. Nikolic, L. Wood, P. A. Eckhoff, R. Langer, G. Traverso, Oral, ultra–long-lasting drug delivery: Application toward malaria elimination goals. *Sci. Transl. Med.* **8**, 365ra157 (2016).
9. P. Nadeau, D. El-Damak, D. Glettig, Y. L. Kong, S. Mo, C. Cleveland, L. Booth, N. Roxhed, R. Langer, A. P. Chandrakasan, G. Traverso, Prolonged energy harvesting for ingestible devices. *Nat. Biomed. Eng.* **1**, 0022 (2017).
10. M. A. Cohen Stuart, W. T. S. Huck, J. Genzer, M. Müller, C. Ober, M. Stamm, G. B. Sukhorukov, I. Szleifer, V. V. Tsukruk, M. Urban, F. Winnik, S. Zauscher, I. Luzinov, S. Minko, Emerging applications of stimuli-responsive polymer materials. *Nat. Mater.* **9**, 101–113 (2010).
11. S. Zhang, A. M. Bellinger, D. L. Glettig, R. Barman, Y.-A. L. Lee, J. Zhu, C. Cleveland, V. A. Montgomery, L. Gu, L. D. Nash, D. J. Maitland, R. Langer, G. Traverso, A pH-responsive supramolecular polymer gel as an enteric elastomer for use in gastric devices. *Nat. Mater.* **14**, 1065–1071 (2015).
12. B. Laulicht, A. Tripathi, V. Schlageter, P. Kucera, E. Mathiowitz, Understanding gastric forces calculated from high-resolution pill tacking. *Proc. Natl. Acad. Sci. U.S.A.* **107**, 8201–8206 (2010).
13. J. Liu, Y. Pang, C. Cleveland, X. Yin, L. Booth, J. Lin, Y.-A. L. Lee, H. Mazdiyasni, S. Saxton, A. R. Kirtane, T. von Erlach, J. Rogner, R. Langer, G. Traverso, Triggerable tough hydrogels for gastric resident dosage forms. *Nat. Commun.* **8**, 124 (2017).
14. C. Steiger, A. Abramson, P. Nadeau, A. P. Chandrakasan, R. Langer, G. Traverso, Ingestible electronics for diagnostics and therapy. *Nat. Rev. Mater.* **4**, 83–98 (2019).
15. M. Mimee, P. Nadeau, A. Hayward, S. Carim, S. Flanagan, L. Jerger, J. Collins, S. McDonnell, R. Swartwout, R. J. Citorik, V. Bulović, R. Langer, G. Traverso, A. P. Chandrakasan, T. K. Lu, An ingestible bacterial-electronic system to monitor gastrointestinal health. *Science* **360**, 915–918 (2018).
16. D. Ruiz, K. Vranas, D. A. Robinson, L. Salvatore, J. W. Turner, T. Addasi, Esophageal perforation after gastric balloon extraction. *Obes. Surg.* **19**, 257–260 (2009).
17. D. V. Jones, C. E. Work, Volume of a swallow. *Am. J. Dis. Child.* **102**, 427 (1961).
18. A. Lendlein, R. Langer, Biodegradable, elastic shape-memory polymers for potential biomedical applications. *Science* **296**, 1673–1676 (2002).
19. K. Bertoldi, V. Vitelli, J. Christensen, M. van Hecke, Flexible mechanical metamaterials. *Nat. Rev. Mater.* **2**, 17066 (2017).
20. S. Babaee, J. Shim, J. C. Weaver, E. R. Chen, N. Patel, K. Bertoldi, 3D soft metamaterials with negative Poisson's ratio. *Adv. Mater.* **25**, 5044–5049 (2013).
21. S. Babaee, J. T. B. Overvelde, E. R. Chen, V. Tournat, K. Bertoldi, Reconfigurable origami-inspired acoustic waveguides. *Sci. Adv.* **2**, e1601019 (2016).
22. A. Cangialosi, C. Yoon, J. Liu, Q. Huang, J. Guo, T. D. Nguyenm, D. H. Gracias, R. Schulman, DNA sequence–directed shape change of photopatterned hydrogels via high-degree swelling. *Science* **357**, 1126–1130 (2017).
23. J. Eatock, G. A. Baker, Managing patient adherence and quality of life in epilepsy. *Neuropsychiatr. Dis. Treat.* **3**, 117–131 (2007).
24. R. M. Jones, J. A. Butler, V. A. Thomas, R. C. Peveler, M. Prevett, Adherence to treatment in patients with epilepsy: Associations with seizure control and illness beliefs. *Seizure* **15**, 504–508 (2006).
25. N. Carral, J. C. Lukas, I. Oteo, E. Suarez, Impact of poor compliance with levofloxacin and moxifloxacin on respiratory tract infection antimicrobial efficacy: A pharmacokinetic/pharmacodynamic simulation study. *Int. J. Antimicrob. Agents* **45**, 79–83 (2015).
26. J. J. Cereghino, J. C. Van Meter, J. T. Brock, J. K. Penry, L. D. Smith, B. G. White, Preliminary observations of serum carbamazepine concentration in epileptic patients. *Neurology* **23**, 357–366 (1973).
27. *Moxifloxacin Hydrochloride* (U.S. Department of Health and Human Services, 2016).
28. Y. Mintz, S. Horgan, J. Cullen, E. Falor, M. A. Talamini, Dual-lumen natural orifice translumenal endoscopic surgery (NOTES): A new method for performing a safe anastomosis. *Surg. Endosc.* **22**, 348–351 (2008).
29. M. Tarnoff, S. Shikora, A. Lembo, Acute technical feasibility of an endoscopic duodenal-jejunal bypass sleeve in a porcine model: A potentially novel treatment for obesity and type 2 diabetes. *Surg. Endosc.* **22**, 772–776 (2008).
30. S. Leary, W. Underwood, R. Anthony, S. Cartner, D. Corey, T. Grandin, C. Greenacre, S. Gwaltney-Brant, M. A. McCrackin, R. Meyer, D. Miller, J. Shearer, R. Yanong, *AVMA Guidelines for the Euthanasia of Animals: 2013 Edition* (American Veterinary Medical Association, 2013).

Acknowledgments: We especially thank C. Cleveland and S. McDonnell for help with the in vivo animal studies; A. Beyzavi and F. Javid for productive discussions and suggestion of thermocouples; A. G. Abramson for help with the x-ray and histology images; A. Lopes for help with HPLC analysis; S. Kim for help with formulation and synthesis of millineedles; K. Vishwanath, T. Hua, and V. Soares for help with mechanical testing and manufacturing and coating; Y. Zhao and S. Zhang for helpful discussion and prototyping of early concepts using shape-memory systems; and all colleagues of the Langer and Traverso laboratories for fruitful discussions. **Funding:** This work was funded in part by the Bill and Melinda Gates Foundation (grant numbers OPP1139921 and OPP1139937) and NIH grant EB000244. **Authors contributions:** S.B., S.P., R.L., and G.T. conceived and designed the research. S.B., S.P., J.S., and G.T. performed the design, mechanical manufacturing, and evaluation. J.E.C., S.T., A.M.H., S.B., S.P., and G.T. performed the in vivo pig experiments. S.B., S.P., A.R.K., E.C.-S., A.V.W., and J.S. performed formulation synthesis and characterization. S.B., S.P., J.S., and E.C.-S. performed linker and elastomer and needle

synthesis and characterization. K.H., A.R.K., and H.M. performed biochemistry analysis. S.B., S.P., R.L., A.R.K., and G.T. discussed and analyzed the results and wrote the manuscript. **Competing interests:** S.B., S.P., J.S., E.C.-S., R.L., and G.T. are co-inventors on provisional application numbers 62/767,749, 62/767,954, and 62/767,798, filed by MIT related to this work. Complete details of all relationships for profit and not for profit for G.T. can be found at the following link: www.dropbox.com/sh/szi7vnr4a2ajb56/AABs5N5i0q9AfT1lqIJAE-T5a?dl=0. For a list of entities with which R.L. is involved, compensated, or uncompensated, see www.dropbox.com/s/yc3xqb5s8s94v7x/Rev%20Langer%20COI.pdf?dl=0. The other authors declare that they have no competing financial interests. **Data and materials availability:** All data associated with this study are present in the paper or the Supplementary Materials.

Submitted 21 July 2018
Resubmitted 13 December 2018
Accepted 22 March 2019
Published 17 April 2019
10.1126/scitranslmed.aau8581

Citation: S. Babaee, S. Pajovic, A. R. Kirtane, J. Shi, E. Caffarel-Salvador, K. Hess, J. E. Collins, S. Tamang, A. V. Wahane, A. M. Hayward, H. Mazdiyasni, R. Langer, G. Traverso, Temperature-responsive biometamaterials for gastrointestinal applications. *Sci. Transl. Med.* **11**, eaau8581 (2019).

Science Translational Medicine

Temperature-responsive biometamaterials for gastrointestinal applications

Sahab Babaee, Simo Pajovic, Ameya R. Kirtane, Jiuyun Shi, Ester Caffarel-Salvador, Kaitlyn Hess, Joy E. Collins, Siddartha Tamang, Aniket V. Wahane, Alison M. Hayward, Hormoz Mazdiyasni, Robert Langer and Giovanni Traverso

Sci Transl Med **11**, eaau8581.
DOI: 10.1126/scitranslmed.aau8581

Shape-shifting drug delivery

Stimuli-responsive biomaterials can be useful for engineering controlled drug delivery systems. Babaee *et al* . designed two orally administered devices to change shape in the presence of warm water. A flower-like device could deliver drug into the upper esophagus via degradable millineedles attached to the "petals" (arms) of the device and could revert to a capsule shape to pass into the stomach in the presence of warm water. A second, flexible macrostructure could deliver large doses of drugs over 2 weeks while residing in the stomach before endoscopically delivered warm water triggered device disassembly via its thermosensitive polymer linkers. Proof-of-concept experiments in pigs reveal the potential of these thermoresponsive drug delivery systems.